A new approach to thermodynamically-consistent models for SMAs

Claudio Giorgi and Angelo Morro

Abstract The paper derives a thermodynamic scheme for SMAs. The new idea of the thermodynamic approach is the formulation of the second law where also the entropy production is given by a constitutive equation. Also by analogy with the usual one-dimensional experimental setting, the paper describes SMAs in a thin parallelepiped form. The body is taken to be subjected to the standard balance equations and the material is characterized by constitutive equations where the temperature, the stress, their time derivatives, and the mass fraction of a phase (martensite) are the variables. The thermodynamic analysis leads to a skeleton surface consisting of equilibrium states and to rate equations governing the evolution of the fields, outside the skeleton surface. It emerges that the rate equations allow a whole account of hysteretic loops induced by temperature or by stress.

1 Introduction

Shape memory alloys (SMAs) are metallic alloys that exhibit a rich variety of hysteretic behaviours. In essence, SMAs show hysteretic effects induced by temperature and stress. Hysteresis is associated with the shape memory effect whereby the body undergoes a change of spatial form. This is due to the fact that the metallic lattice has two different equilibrium configurations, one is the high-symmetric high-temperature austenite and the other is the low-temperature martensite.

The practical interest arising from the shape memory is accompanied by the concern into the mathematical models of hysteretic phenomena induced by both

Claudio Giorgi
Dipartimento di Ingegneria Civile Ambiente Territorio Architettura e Matematica, Università di Brescia, Via Valotti 9, 25133 Brescia, Italy. e-mail: claudio.giorgi@unibs.it

Angelo Morro
Dipartimento di Informatica, Bioingegneria, Robotica e Ingegneria dei Sistemi, Università di Genova, Via All'Opera Pia 13, 16145 Genoa, Italy. e-mail: angelo.morro@unige.it

temperature and stress. A reasonable report on the literature on SMAs is given by recent review papers on the subject; among them we mention [1, 2, 3] while further references on the subject are [4, 5, 6, 7].

Many works are based on microscopic models with various potential energies of interaction between particles. Other approaches of macroscopic character have been developed where the main technical point is the evolution equation for the mass fraction ξ of a phase [3]. Often suitable internal variables are associated with the deformation and then the scheme is completed through corresponding thermodynamic forces [8]. Thermodynamic approaches have been developed by modelling the mass fraction as a phase change variable (e.g. [9]) or an order parameter (e.g. [10]) and accordingly introducing a generalized thermodynamic force in the balance equations.

Physically-admissible models are required to be thermodynamically consistent. Furthermore, a systematic thermodynamic approach should simplify the description of a material by using a few constitutive functions possibly without introducing additional forces and powers and hence changing the balance equations. With this idea, a recent approach of ours allows the formulation of thermodynamically-consistent models of hysteresis in terms of free energy and entropy production (see, e.g., [11, 12]).

The new idea of our approach is to regard the entropy production as a constitutive function per se, just as it happens for all of the constitutive functions. It is apparent that this feature results in more general schemes. Technically, this allows the formulation of rate equations where the entropy production is a non-negative valued function of the variables under consideration (see, e.g., [13]).

Also in view of the usual one-dimensional experimental setting, in this paper we describe SMAs in a thin parallelepiped form with the stress applied in the longitudinal direction. The body is taken to obey the standard balance equations and the material is characterized by constitutive equations where the temperature, the stress, their time derivatives, and the mass fraction of a phase (martensite) are the variables. The purpose is to derive from thermodynamics a scheme where both equilibrium states and evolution equations are established. The scheme is expected to describe equilibrium states, evolutions and, in particular, hysteretic loops induced by temperature or by stress.

2 Notation and balance equations

The body occupies a time-dependent three-dimensional region Ω; we let Ω be in a parallelepiped form $\Omega = \{I \times S\}$ where I is a segment and S is a square orthogonal to I. The position vector of a point in Ω is denoted by $\mathbf{x}$. The symbol ∇ denotes the gradient while $\nabla\cdot$ is the divergence operator.

The motion is specified by a function $\mathbf{x} = \boldsymbol{\chi}(\mathbf{X}, t)$, where $\mathbf{X}$ is the position vector of the point in a reference configuration R. Hence formally we can write $\Omega = \boldsymbol{\chi}(\mathrm{R}, t)$. The symbol $\mathbf{F}$ denotes the deformation gradient, in suffix notation $F_{iK} = \partial_{X_K}\chi_i$. The

symbol $f(\mathbf{x},t)$ denotes the value of f at $\mathbf{x}$, at time $t \in \mathbb{R}$. The symbols $\partial_t, \partial_{x_i}, \partial_{X_K}$ denote partial derivatives. Hence $\mathbf{v} = \partial_t \boldsymbol{\chi}(\mathbf{X},t)$ is the velocity. A superposed dot denotes the total time derivative so that for $f(\mathbf{x},t)$ it is $\dot{f} = \partial_t f + (\mathbf{v}\cdot\nabla)f$.

Let ρ be the mass density. The conservation of mass is expressed locally in the form

$$\dot{\rho} + \rho\nabla\cdot\mathbf{v} = 0.$$

If $J = \det\mathbf{F} > 0$ then it follows that

$$\rho J = \rho_R,$$

$\rho_R(\mathbf{X})$ being the mass density in the reference configuration.

The equation of motion is written in the form

$$\rho\dot{\mathbf{v}} = \nabla\cdot\mathbf{T} + \rho\mathbf{b},$$

where $(\nabla\cdot\mathbf{T})_i = \partial_{x_j}T_{ij}$ and $\mathbf{b}$ is body force density. Also, $\mathbf{T}$ is the Cauchy stress tensor; by the balance of angular momentum we have $\mathbf{T} = \mathbf{T}^T$.

Let $\mathbf{L}$ be the velocity gradient, $L_{ij} = \partial_{x_j}v_i$, and $\mathbf{D}$ the stretching tensor, namely $\mathbf{D} = \mathrm{sym}\mathbf{L}$. Denote by ε the internal energy density, $\mathbf{q}$ the heat flux vector and r the energy supply. The balance of energy leads to

$$\rho\dot{\varepsilon} = \mathbf{T}\cdot\mathbf{D} - \nabla\cdot\mathbf{q} + \rho r. \tag{1}$$

Let θ be the absolute temperature, η the specific entropy density, $\mathbf{j}$ the entropy flux, and r/θ the entropy supply. The balance of entropy leads to

$$\rho\dot{\eta} + \nabla\cdot\mathbf{j} - \frac{\rho r}{\theta} = \rho\gamma,$$

where γ is the (rate of) entropy production.

A process $\mathcal{P}$ is the set of fields entering the balance equations. As with recent applications of ours, we let γ be given by a constitutive function. Physically admissible sets of constitutive functions are required to satisfy the second law of thermodynamics in the following form.

Postulate. For every process $\mathcal{P}$ admissible in a body the inequality

$$\rho\dot{\eta} + \nabla\cdot\mathbf{j} - \frac{\rho r}{\theta} = \rho\gamma \geq 0, \tag{2}$$

is valid at any internal point.

Henceforth eq. (2) is referred to as Clausius-Duhem (CD) inequality. Let $\mathbf{j} = \mathbf{q}/\theta + \mathbf{k}$. Substitute $\nabla\cdot\mathbf{q} - \rho r$ from (1) into (2) to obtain

$$-\rho(\dot{\psi} + \eta\dot{\theta}) + \mathbf{T}\cdot\mathbf{D} + \theta\nabla\cdot\mathbf{k} - \frac{1}{\theta}\mathbf{q}\cdot\nabla\theta = \rho\theta\gamma, \tag{3}$$

where $\psi = \varepsilon - \theta\eta$ is the Helmholtz free energy.

The following scheme holds with $\mathbf{k} = \mathbf{0}$. Nonzero $\mathbf{k}$ occur in connection with nonlocal properties expressed by gradients of the variables. Hereafter it is understood and not written that $\gamma \geq 0$.

3 One-dimensional thermodynamic scheme for SMAs

Consider Ω in the parallelepiped form $\Omega = I \times S$ with $I = [0, l(t)]$. We let $x \in [0, \infty)$ be the variable along the axis comprising I and $X \in [0, l(0)]$. The deformation gradient $\mathbf{F}$ is diagonal and we let $F = \partial_X x > 0$. Let $L = \partial_x v$ be the velocity gradient in the chosen x-direction; hence $L = \dot{F}F^{-1}$.

Let σ be the traction in the x-direction while the other entries of $\mathbf{T}$ are zero. Hence the surface $I \times \partial S$ is traction free. We let $J = \det \mathbf{F}$. In view of the diagonal structure of $\mathbf{F}$ we can write

$$J = FF_\perp^2,$$

where $F_\perp$ is the common value of $\mathbf{F}$ at the lateral faces. The product $J\rho$ is the referential mass density, say ρ_R. While in general ρ_R can depend only on the position we assume that ρ_R is independent of $\mathbf{X}$ and hence is constant. For simplicity we neglect heat conduction ($\mathbf{q} = \mathbf{0}$) and the CD inequality (3) can be written in the form

$$-\rho(\dot{\psi} + \eta\dot{\theta}) + \sigma\dot{F}F^{-1} = \rho\theta\gamma. \tag{4}$$

Define $h = \ln F$. Hence it follows

$$-\rho(\dot{\psi} + \eta\dot{\theta}) + \sigma\dot{h} = \rho\theta\gamma.$$

The crucial property of SMAs is the transformation between austenite and martensite. In this paper we confine our attention to positive-oriented (or detwinned) martensite which occurs when the values of both absolute temperature θ and tensile stress σ are not too small. The single-martensite model has often been chosen for a detailed study because of its simplicity and ease of experimental verification [1]. To describe the related properties we use the (martensitic) phase fraction ξ,

$$\xi = \frac{\rho_M}{\rho_A + \rho_M},$$

ρ_A, ρ_M being the mass densities of austenite and martensite.

Multiply (4) by J and let $J\sigma = \tau$ to obtain

$$-\rho_R(\dot{\psi} + \eta\dot{\theta}) + \tau\dot{h} = \rho_R\theta\gamma. \tag{5}$$

Let

$$\phi = \psi - \frac{1}{\rho_R}\tau h. \tag{6}$$

Hence the CD inequality (5) can be written in the form

$$-\rho_R(\dot{\phi} + \eta\dot{\theta}) - h\dot{\tau} = \rho_R\theta\gamma. \tag{7}$$

We append some comments on the modelling of h and η and the definitions of τ and ϕ. By analogy with the literature (e.g. [2]), we assume h and η are given by the additive decompositions

$$h = h^e + h^{tr}, \qquad \eta = \eta^e + \eta^{tr}. \tag{8}$$

The terms h^e and η^e are then viewed as strain and entropy and are assumed to arise from an energy potential, as with elastic solids, though here h^e and η^e can depend also on the mass fraction ξ. The quantities h^{tr} and η^{tr} (often called transition or transformation functions) are additional terms related to the presence of austenite and martensite and arise from the transformation mechanism between the two phases.

By the Nanson formula ([14], p. 20; [15], p. 71) the current surface element $\mathbf{n}\,da$ and the corresponding reference surface element $\mathbf{n}_R da_R$ are related by

$$\mathbf{n}\,da = J\mathbf{F}^{-T}\mathbf{n}_R da_R.$$

Since $\mathbf{T} = \sigma\mathbf{n}\otimes\mathbf{n}$, and $\mathbf{F}$ is diagonal, then $\mathbf{n} = \mathbf{n}_R$ and

$$da = JF^{-1}da_R.$$

If we denote by σ_R the reference stress we have $\sigma\,da = \sigma_R da_R$, whence

$$\sigma_R = JF^{-1}\sigma.$$

This relation is consistent with the definition of the first Piola stress tensor ([16], ch. 24; [17], p. 94)

$$\mathbf{T}_R = J\mathbf{T}\mathbf{F}^{-T}$$

as the stress in the reference configuration. Instead,

$$\tau = J\sigma$$

is merely the $\mathbf{n}$-component of the Kirchhoff stress $\mathbf{T}_K = J\mathbf{T}$.

In connection with (6) we observe that, in classical thermodynamics, $\phi = \psi + p/\rho$ is the specific Gibbs free energy (or total free energy if the kinetic energy is included in $\varepsilon = \psi + \theta\eta$ [18]). Since $\tau/\rho_R = \sigma/\rho$ then, relative to the Gibbs free energy, the present function ϕ is a modified Gibbs free energy with the mechanical term $-\sigma h/\rho$ in place of p/ρ. This definition is motivated directly by the balance of entropy (4).

4 Thermodynamic restrictions

The expected evolution equation is thought as a relation among $\dot{\xi}, \dot{\tau}, \dot{\theta}$, possibly with $\dot{\xi}$ as a function of $\dot{\tau}, \dot{\theta}$ and θ, τ, ξ. This suggests that we let

$$\theta, \tau, \xi, \dot{\theta}, \dot{\tau}$$

be the variables. Hence ϕ, h, η, γ, and $\dot{\xi}$ are taken to be given by constitutive functions. Indeed h, η, γ, and $\dot{\xi}$ are given by continuous functions while ϕ is continuously differentiable. Upon computation of $\dot{\phi}$ we can write the CD inequality (7) in the form

$$-\rho_R(\partial_\theta\phi + \eta)\dot{\theta} - (\rho_R\partial_\tau\phi + h)\dot{\tau} - \rho_R\partial_\xi\phi\,\dot{\xi} - \rho_R\partial_{\dot{\theta}}\phi\ddot{\theta} - \rho_R\partial_{\dot{\tau}}\phi\ddot{\tau} = \rho_R\theta\gamma. \quad (9)$$

The linearity and arbitrariness of $\ddot{\theta}$ and $\ddot{\tau}$ imply

$$\partial_{\dot{\theta}}\phi = 0, \qquad \partial_{\dot{\tau}}\phi = 0.$$

In dealing with a thermoelastic solid we would find that $\eta = -\partial_\theta\phi$, $h = -\partial_\tau\phi$. By analogy we let

$$\eta^e = -\partial_\theta\phi, \qquad h^e = -\rho_R\partial_\tau\phi. \quad (10)$$

Consequently the functions η^{tr}, h^{tr} and $\dot{\xi}$ are required to satisfy the reduced inequality

$$-\rho_R\eta^{tr}\dot{\theta} - h^{tr}\dot{\tau} - \rho_R\partial_\xi\phi\,\dot{\xi} = \rho_R\theta\gamma. \quad (11)$$

By the general constitutive assumption, the entropy production γ is a function of $\theta, \tau, \xi, \dot{\theta}, \dot{\tau}$. Instead, it is $\phi = \phi(\theta, \tau, \xi)$. Likewise, and also in connection with experimental data [19], we let both η^{tr} and h^{tr} be functions of θ, τ, ξ.

In the following sections we will see that eq. (11) gives a full description of the one-dimensional martensitic phase transitions. Indeed, upon suitable selections of the functions ϕ, h^{tr}, η^{tr} and γ, eq. (11) determines the hysteretic loops related to the austenite $\leftrightarrows$ martensite transformations.

Since we are considering a single variant of martensite, we confine our attention to the temperature-stress domain

$$\mathcal{D} = \{(\theta, \tau) : \theta \geq \hat{\theta}_M > 0\}.$$

In fact, for temperatures below $\hat{\theta}_M$, the material is always in the martensitic phase (twinned, mixed or detwinned). The introduction of a phase transition temperature $\hat{\theta}_M$ is not new in the literature (see, e.g., Fig. 1.a of [3] where M_f^0 stands for $\hat{\theta}_M$). In particular, $\hat{\theta}_M \simeq 200^\circ$ K for NiTi-based single crystals (see, e.g., [20]).

4.1 Isothermal cyclic processes

Further consequences follow in connection with closed thermodynamic processes as it happens with hysteretic loops. At isothermal processes ($\dot{\theta} = 0$) eq. (11) simplifies to

$$-\rho_R\dot{\phi} - h\dot{\tau} = \rho_R\theta\gamma, \quad (12)$$

while ϕ, h, and γ are given by functions of the form $\hat{\phi}(\tau,\xi)$, $\hat{h}(\tau,\xi,\dot{\tau})$, $\hat{\gamma}(\tau,\xi,\dot{\tau})$. Let $(\tau(t),\xi(t)) : \mathbb{R} \to \mathbb{R}^2$ be a closed function on $[0,T]$, namely $\tau(T) = \tau(0), \xi(T) = \xi(0)$. Hence $\phi(t) = \hat{\phi}(\tau(t),\xi(t))$ satisfies $\phi(T) = \phi(0)$. Since $\gamma \geq 0$ then integrating (12) on $[0,T]$ we find

$$\int_0^T h\dot{\tau}dt = -\rho_R\theta \int_0^T \gamma(t)dt \leq 0.$$

Denote by C_τ the closed curve $C_\tau : t \mapsto (\tau(t), h(t))$, $\tau(T) = \tau(0), h(T) = h(0)$. Hence

$$\int_{C_\tau} hd\tau = \int_0^T h\dot{\tau}dt \leq 0.$$

Consequently the closed curve C_τ is oriented in the counterclockwise sense, in the $\tau - h$ plane, and

$$\mathcal{A}_\tau = \rho_R\theta \int_0^T \gamma(t)dt$$

is the positive area bounded by C_τ. However, in the most natural strain-stress plane the overturned closed curve $\tilde{C}_\tau$ is oriented in the clockwise sense as depicted in the schematic Fig. 1 below inspired by Fig. 1.b of reference [3].

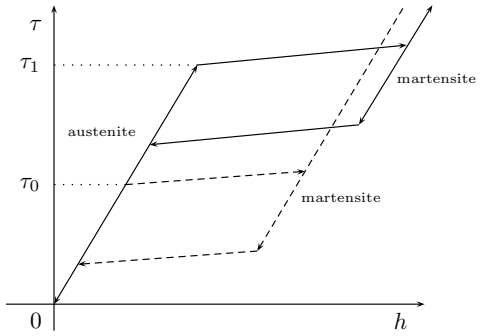

Fig. 1 Schematic major hysteresis loops in the strain-stress plane at constant temperature: θ_0 (dashed) and $\theta_1 > \theta_0$ (solid).

In Fig. 1 we implicitly assume $\theta_0 \geq \hat{\theta}_A$, where $\hat{\theta}_A$ represents the final temperature of an austenitic transformation during heating in a stress-free state and corresponds to A_f^0 in [3, Fig. 1.a]. Since the transformation temperatures are sensitive to small alloy composition changes, in commercial NiTi-based alloys $\hat{\theta}_A$ covers a range from approximately 250 to 400° K (see, e.g., [21]). Moreover, τ_0 and τ_1 denote the starting stresses of a martensitic transformation at temperatures θ_0 and θ_1, respectively. This means that $\tau_0 = \tau_M^s(\theta_0)$ and $\tau_1 = \tau_M^s(\theta_1)$, as can be seen from the subsequent Fig. 2.

Likewise look at processes with $\dot{\tau} = 0$. We can then write eq. (11) in the form

$$-\dot{\phi} - \eta\dot{\theta} = \theta\gamma,$$

where ϕ is a function of θ, ξ while η, γ are functions of $\theta, \xi, \dot{\theta}$. As $t \in [0, T]$ the image $(\theta(t), \eta(t))$ yields the closed curve C_θ. Hence we have

$$\int_{C_\theta} \eta d\theta = \int_0^T \eta\dot{\theta} dt = -\int_0^T \theta\gamma dt \leq 0.$$

Thus

$$\int_{C_\theta} \eta d\theta = -\mathcal{A}_\theta,$$

where $\mathcal{A}_\theta$ is the (positive) area bounded by C_θ. The negative value of the integral denotes that C_θ is run counterclockwise in the $\theta - \eta$ plane. Thus, closed curves in the stress-strain and temperature-entropy planes are oriented counterclockwise. Unfortunately, loops of this type are usually neither studied nor represented in the SMA literature. However, temperature-entropy hysteresis loops are described in a recent papers on first-order transitions in magnetocaloric materials [22].

4.2 Mass fraction loops

For cycles involving the mass fraction ξ, no direct conclusion follows directly from thermodynamics. In order to develop a simple but complete model, it is however reasonable to assume that both the logarithmic deformation h and the entropy $\rho_R\eta$ linearly depend on ξ.

If h is assumed in the form

$$h = \kappa(\tau, \theta) + \lambda(\tau)\xi, \tag{13}$$

then, along cyclic isothermal processes,

$$0 \geq \int_0^T h\dot{\tau} dt = \int_0^T \hat{\kappa}(\tau)\dot{\tau} dt + \int_0^T \xi\lambda(\tau)\dot{\tau} dt,$$

where $\hat{\kappa}$ denote the function κ at constant temperature. Consider the closed curve $C^\dagger : t \to (\tau(t), \xi(t)), \tau(T) = \tau(0), \xi(T) = \xi(0)$. If $0 < \bar{\lambda} \leq \lambda(\tau)$ then we have

$$\bar{\lambda} \int_{C^\dagger} \xi d\tau \leq \int_{C^\dagger} \xi\lambda(\tau) d\tau \leq 0.$$

Hence the closed curve $C^\dagger$ in the $\tau - \xi$ plane is oriented counterclockwise (see Fig. 2), which is consistent with experimental data (see, e.g., [23]). Since $\lambda(\tau) = h_{\xi=1} - h_{\xi=0}$, then $\lambda(\tau)$ equals the variation of h due to a complete phase change at a fixed stress τ.

Likewise, assume the entropy is given in the form

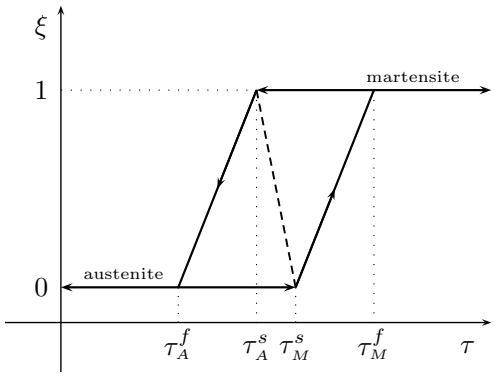

Fig. 2 Schematic description of the stress-induced transition. Major hysteresis loop of the martensite concentration ξ as a function of the stress τ at constant temperature $\theta = \theta_0 > \hat{\theta}_A$.

$$\rho_R \eta = \ell(\tau, \theta) - \mu(\theta)\xi, \tag{14}$$

and consider the closed curve $C^\ddagger : t \longrightarrow (\theta(t), \xi(t)), \theta(T) = \theta(0), \xi(T) = \xi(0)$. Along cyclic processes at constant stress, $\tau = \tau_0$, by (7) and (14) it follows that

$$0 \geq \rho_R \int_0^T \eta\dot{\theta}dt = \int_0^T \hat{\ell}(\theta)\dot{\theta}dt - \int_0^T \xi\mu(\theta)\dot{\theta}dt,$$

where $\hat{\ell}(\theta) = \ell(\tau_0, \theta)$. Let $0 < \mu(\theta) \leq \hat{\mu}$. It follows that

$$\hat{\mu} \int_{C^\ddagger} \xi d\theta \geq \int_{C^\ddagger} \xi\mu(\theta)d\theta \geq 0. \tag{15}$$

Hence the closed curve $C^\ddagger$ in the $\theta - \xi$ plane is oriented clockwise (see Fig. 3), which is consistent with experimental data (see, e.g., [24, ch. 1]) that show the condition $\dot{\theta}\dot{\xi} \leq 0$. Since $\mu(\theta) = \rho_R(\eta_{\xi=0} - \eta_{\xi=1})$, then $\mu(\theta)$ equals the variation of entropy $\rho_R\eta$ due to a complete phase change at a fixed temperature θ.

5 Constitutive assumptions

We now derive a thermodynamically consistent model by choosing appropriate functional expressions for the Gibbs free energy, ϕ, the transition functions, η^{tr}, h^{tr} and the entropy production function, γ.

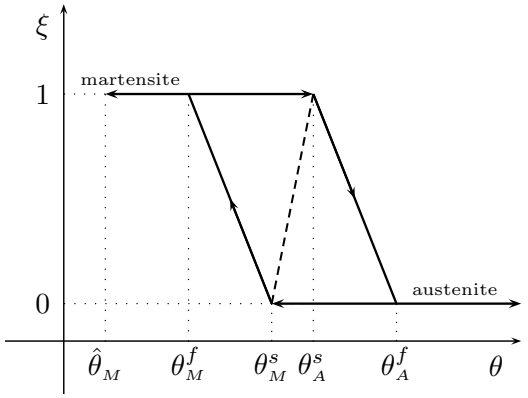

Fig. 3 Schematic description of the temperature-induced transition. Major hysteresis loop of the martensite concentration ξ as a function of the temperature θ at constant stress $\tau = \tau_0 > \tau_*$.

5.1 Gibbs free energy

First, we look for a Gibbs free energy ϕ consistent with (13) and (14). Assume $\rho_R\phi$ in the simple form (quadratic in ξ)

$$\rho_R\phi = \mathcal{G}(\tau,\theta) - \tfrac{1}{2}\alpha\xi^2 + [\mathcal{S}(\theta) - \mathcal{T}(\tau)]\xi, \tag{16}$$

where α is a constant and $\mathcal{G}(\tau,\theta)$ represents the Gibbs free energy of the austenite. In view of (13) and (14), we let

$$\alpha > 0, \quad \mathcal{S}'(\theta) > 0, \quad \mathcal{T}'(\tau) \geq \bar{\lambda} > 0, \quad \mathcal{S}(0) = 0, \quad \mathcal{T}(0) = 0. \tag{17}$$

From (16) we have

$$\rho_R\partial_\xi\phi = -\alpha\xi + \mathcal{S}(\theta) - \mathcal{T}(\tau), \tag{18}$$

$$\rho_R\partial_\theta\phi = \partial_\theta\mathcal{G}(\tau,\theta) + \mathcal{S}'(\theta)\xi, \quad \rho_R\partial_\tau\phi = \partial_\tau\mathcal{G}(\tau,\theta) - \mathcal{T}'(\tau)\xi.$$

Consequently, from definitions (10) it follows

$$\begin{aligned} \rho_R\eta^e &= -\rho_R\partial_\theta\phi = -\partial_\theta\mathcal{G}(\tau,\theta) - \mathcal{S}'(\theta)\xi, \\ h^e &= -\rho_R\partial_\tau\phi = -\partial_\tau\mathcal{G}(\tau,\theta) + \mathcal{T}'(\tau)\xi. \end{aligned} \tag{19}$$

5.2 Transition functions

For definiteness in later developments we assume the following expressions of the transition functions

$$\eta^{tr} = k(\theta)\partial_\xi\phi, \qquad h^{tr} = p(\tau)\rho_R\partial_\xi\phi, \tag{20}$$

with the functions $k(\theta)$ and $p(\tau)$ to be determined. By virtue of (18), it follows that

$$\begin{aligned} \rho_R \eta^{tr} &= -k(\theta)[\alpha\xi - \mathcal{S}(\theta) + \mathcal{T}(\tau)], \\ h^{tr} &= -p(\tau)[\alpha\xi - \mathcal{S}(\theta) + \mathcal{T}(\tau)]. \end{aligned} \tag{21}$$

To determine the connections with κ, λ, ℓ, and μ appearing in (13) and (14) we observe that

$$\rho_R \eta = \rho_R(\eta^e + \eta^{tr}) = -[\alpha k(\theta) + \mathcal{S}'(\theta)]\xi - \partial_\theta \mathcal{G}(\tau,\theta) + k(\theta)[\mathcal{S}(\theta) - \mathcal{T}(\tau),$$

$$h = h^e + h^{tr} = [\mathcal{T}'(\tau) - \alpha p(\tau)]\xi - \partial_\tau \mathcal{G}(\tau,\theta) + p(\tau)[\mathcal{S}(\theta) - \mathcal{T}(\tau)]. \tag{22}$$

Hence, a comparison with (14) and (13) yields

$$\mu(\theta) = \alpha k(\theta) + \mathcal{S}'(\theta), \qquad \ell(\tau,\theta) = -\partial_\theta \mathcal{G}(\tau,\theta) + k(\theta)[\mathcal{S}(\theta) - \mathcal{T}(\tau)],$$

$$\lambda(\tau) = \mathcal{T}'(\tau) - \alpha p(\tau), \qquad \kappa(\tau,\theta) = -\partial_\tau \mathcal{G}(\tau,\theta) + p(\tau)[\mathcal{S}(\theta) - \mathcal{T}(\tau)].$$

Consistency with the results on the orientation of closed curves obtained in Sect. 4.2 holds if

$$\mathcal{T}'(\tau) - \alpha p(\tau) \geq \bar{\lambda} > 0, \quad \mathcal{S}'(\theta) + \alpha k(\theta) > 0.$$

By virtue of (17), these conditions are satisfied provided only that $k(\theta) > 0$ and $p(\tau) < 0$. For formal convenience we then let

$$p(\tau) = -\varkappa(\tau), \quad \varkappa(\tau) > 0$$

and h^{tr} can rewritten as

$$h^{tr} = \varkappa(\tau)[\alpha\xi - \mathcal{S}(\theta) + \mathcal{T}(\tau)]. \tag{23}$$

One might introduce expressions for the free energy ϕ that are more involved than (16). For example, quite a general expression for ϕ might be

$$\rho_R \phi = \mathcal{G}(\tau,\theta) - \Xi(\xi) + [\mathcal{S}(\theta) - \mathcal{T}(\tau)]\Xi'(\xi),$$

where $\Xi'(\xi)\xi > 0$. Unfortunately, the corresponding expressions for h and η would no longer be linear in ξ and the term $\alpha\xi$ would be replaced with $\Xi'(\xi)$ in equations (21) and in the following ones. Hence, for a more direct illustration of the method, hereafter we consider $\rho_R\phi$ in the form (16).

5.3 Entropy production

The functions η^{tr}, h^{tr} are represented by (21), (23) and are required to satisfy the reduced dissipation inequality (11). In this connection we complete the scheme by

assuming the entropy production in the form

$$\theta\gamma = g(\xi)|\partial_\xi\phi|\big[\beta(\theta)|\dot\theta| + \nu(\tau)|\dot\tau|\big], \tag{24}$$

where g, β and ν are positive functions. Hence, by virtue of (20), eq. (11) can be written in the form

$$-\partial_\xi\phi k(\theta)\dot\theta + \partial_\xi\phi\varkappa(\tau)\dot\tau - \partial_\xi\phi\dot\xi = g(\xi)|\partial_\xi\phi|\big[\beta(\theta)|\dot\theta| + \nu(\tau)|\dot\tau|\big], \tag{25}$$

If $\partial_\xi\phi \neq 0$ then (25) reduces to a rate-type equation that determines the evolution of $\xi(t)$ induced by $\theta(t)$ and $\tau(t)$. Indeed, by virtue of (18),

$$k(\theta)\dot\theta - \varkappa(\tau)\dot\tau + \dot\xi = g(\xi)\,\mathrm{sgn}\big[\alpha\xi - \mathcal{S}(\theta) + \mathcal{T}(\tau)\big]\big[\beta(\theta)|\dot\theta| + \nu(\tau)|\dot\tau|\big]. \tag{26}$$

At constant stress, say $\tau = \tau_0$, $\dot\tau = 0$, eq. (26) simplifies to

$$\dot\xi = -k(\theta)\dot\theta + \beta(\theta)g(\xi)\,\mathrm{sgn}[\alpha\xi - \mathcal{S}(\theta) + \mathcal{T}(\tau_0)]|\dot\theta|, \tag{27}$$

a hysteretic Duhem model describing temperature-induced transitions. If instead the temperature is constant, say $\theta = \theta_0$, $\dot\theta = 0$, then

$$\dot\xi = \varkappa(\tau)\dot\tau + \nu(\tau)g(\xi)\ \mathrm{sgn}[\alpha\xi - \mathcal{S}(\theta_0) + \mathcal{T}(\tau)]|\dot\tau| \tag{28}$$

provides the corresponding hysteretic Duhem model of stress-induced transitions.

It is worth remarking that eq.(26) is the general nonlinear model equation for the one-dimensional evolution of a SMA when nonlocal effects are neglected. The formulation of a three-dimensional model that also describes non-local aspects will be considered in a future contribution.

As we show in the next sections, particular cases of eqs. (27) and (28) allow a direct closed-form determination of the time functions $\theta(t), \tau(t), \xi(t)$.

6 Evolution equations and hysteresis loops

In this section we apply the previous thermodynamic results and establish an operative description of the evolution of the temperature, stress, and mass fraction in SMAs. Based on the thermodynamic relation (26) we look for an operative though qualitative scheme without fitting data of particular alloys.

6.1 Equilibrium surface and its projections

We start by looking for the modelling functions $\mathcal{S}(\theta), \mathcal{T}(\tau)$ so that they are consistent with the observed hysteretic properties of the transitions. If $\partial_\xi\phi \neq 0$ then eq. (25) determines an evolution equation involving $\theta(t), \tau(t), \xi(t)$. If instead $\partial_\xi\phi = 0$ then

we have

$$\alpha\xi - \mathcal{S}(\theta) + \mathcal{T}(\tau) = 0, \tag{29}$$

which characterizes equilibrium states (θ, τ, ξ) of the alloy. Indeed, from (24), it follows $\gamma = 0$. We then refer to (29) as the *equilibrium surface* and we can read it from two different points of view. First, for any given pair (θ, τ) eq. (29) determines the equilibrium fraction ξ. Second, for any given martensitic fraction ξ it gives a curve in the $\theta-\tau$ plane representing the temperature-stress equilibrium values. Since the martensite fraction is subject to the constraint $\xi \in [0, 1]$, the projection of the equilibrium surface on the $\theta - \tau$ plane is

$$\mathcal{E} = \{(\theta, \tau) : 0 \leq \mathcal{S}(\theta) - \mathcal{T}(\tau) \leq \alpha\}.$$

For definiteness hereafter we let $\mathcal{S}(\theta)$ and $\mathcal{T}(\theta)$ be linear in that

$$\mathcal{S}(\theta) = c_\theta\, \theta + d_\theta, \qquad \mathcal{T}(\tau) = c_\tau\, \tau + d_\tau,$$

where c_θ and c_τ are positive constants by virtue of (17). Hence eq. (29) is taken in the form

$$\alpha\xi = c_\theta\theta - c_\tau\tau + c_d, \quad c_d = d_\theta - d_\tau, \tag{30}$$

and represents the set of all possible equilibrium states (θ, τ, ξ). Letting

$$m = c_\theta/c_\tau > 0, \qquad \tau_d = c_d/c_\tau, \qquad q = \alpha/c_\tau > 0,$$

and accounting for $0 \leq \xi \leq 1$, the region $\mathcal{E}$ is represented by the strip

$$0 \leq m\theta - \tau + \tau_d \leq q.$$

We now examine the relationship between the material parameters introduced so far and the parameters characterizing the schematic hysteretic loops depicted in Figs. 2 and 3. To this end we consider the projection of the equilibrium surface on the planes $\theta = \theta_0$ or $\tau = \tau_0$.

At constant temperature, $\theta = \theta_0$, the projection of (30) results in a segment in the $\tau - \xi$ plane, namely

$$\alpha\xi = c_\theta\theta_0 - c_\tau\tau + c_d, \quad 0 \leq \xi \leq 1.$$

In Fig. 2 this segment is represented by a dashed line, sometimes referred to as 'skeleton curve' of the cycle. In light of this schematic picture, as $\xi = 0$ or $\xi = 1$ we obtain the values

$$\tau^s_M|_{\theta=\theta_0} = m\theta_0 + \tau_d, \qquad \tau^s_A|_{\theta=\theta_0} = m\theta_0 + \tau_d - q.$$

On the other hand, at constant stress, $\tau = \tau_0$, the projection of (30) yields (see the dashed line in Fig. 3)

$$\alpha\xi = c_\theta\theta - c_\tau\tau_0 + c_d, \quad 0 \leq \xi \leq 1,$$

whence, at $\xi = 0$ and $\xi = 1$, we have

$$\theta_M^s|_{\tau=\tau_0} = (\tau_0 - \tau_d)/m, \qquad \theta_A^s|_{\tau=\tau_0} = (q + \tau_0 - \tau_d)/m. \tag{31}$$

In particular we let

$$\theta_\dagger := \theta_A^s|_{\tau=0} = (q - \tau_d)/m \tag{32}$$

Accordingly, the upper boundary of the equilibrium strip, namely (see Fig. 4)

$$r_u = \{(\theta, \tau) : \tau = m\theta + \tau_d\},$$

can be viewed as the set of temperature-stress pairs at which a martensitic transition starts when the evolution process leaves the equilibrium set $\mathcal{E}$, whereas its lower boundary, namely

$$r_\ell = \{(\theta, \tau) : \tau = m\theta + \tau_d - q\},$$

represents the set of temperature-stress pairs at which an austenitic transition starts.

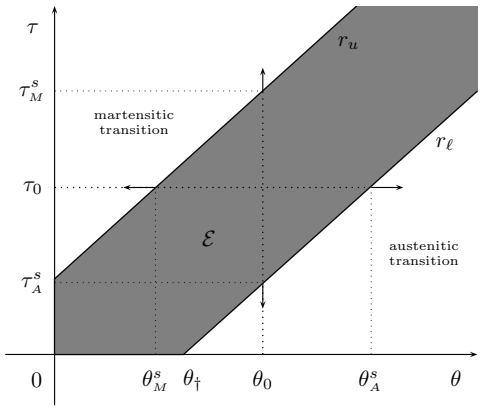

Fig. 4 Schematic diagram of the starting points of the martensitic and austenitic transition at constant stress, $\tau = \tau_0$, or constant temperature, $\theta = \theta_0$.

6.2 Schematic representation of the phase transition diagram

At low stress, however, experimental data suggest that the onset temperature of a martensitic transformation during cooling remains nearly constant [20]. Let

$$\theta_* = \theta_M^s|_{\tau=0}$$

be the starting temperature of a martensitic transformation during cooling in a stress-free state. The evolution of θ_M^s as the tensile stress increases ($\tau > 0$) is described in

Fig.3 of [20]. With a good approximation we can represent this evolution with the piecewise-linear dashed curve in Fig. 5: the value of θ_M^s remains equal to θ_* (M_s^0 in [20]) until the stress reaches a threshold value τ_* ($\sigma_{\rm cr}(M_s^0)$ in [20]) and then assumes a linear trend. According to experimental data concerning NiTi-based SMAs, also called Nitinol, we infer that

$$\theta_* \simeq 225^\circ\mathrm{K} > \hat\theta_M, \qquad \tau_* \simeq 125\,\mathrm{MPa}$$

and the slope $1/m$ is proportional to the strain of the CVP (corresponding variants pairs)-structure formation of the SMA (see [20] Section 4).

Accordingly, Figure 5 provides a schematic but complete representation of the phase transition diagram for a SMA (to be compared, e.g., with Fig. 1a of [3]). Observe that all possible mixed states (austenite + martensite with $\xi \in (0,1)$) are allowed in the equilibrium region (see the dark grey strip in Fig. 5)

$$\mathcal{E}_* = \{(\theta,\tau):\ \theta \geq \theta_*,\ \tau \in [m\theta + \tau_d - q, m\theta + \tau_d]\}.$$

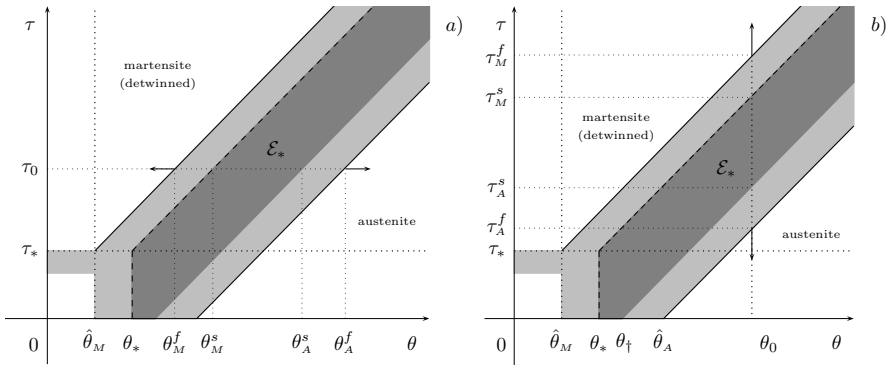

Fig. 5 Schematic $\theta - \tau$ phase diagram: (a) temperature-induced transition ($\tau = \tau_0 > \tau_*$); (b) stress-induced transition ($\theta = \theta_0 > \hat\theta_A$).

Since it is required that $\tau_* = m\theta_* + \tau_d$ we infer that

$$\tau_d = \tau_* - m\theta_*. \tag{33}$$

(τ_d is negative in Fig. 5). Moreover, by (32) we have

$$q = \tau_* + m(\theta_\dagger - \theta_*) \tag{34}$$

The two light grey bands in Fig. 5, instead, represent transition temperature-stress values in which the martensite concentration ξ lies in a neighborhood of 0 (the lower band) or 1 (the upper band). We now look for determining the values of θ_M^f, θ_A^f

and τ_M^f, τ_A^f. Indeed, the upper and lower contours of the above bands consist of the collection of all pairs (θ_M^f, τ_M^f) and (θ_A^f, τ_A^f) respectively.

Consider first the evolution, at constant stress τ_0, i.e. $(\theta(t), \xi(t))$ as $t \in [0, T]$ such that

$$\xi(0) = 0,\ \xi(T) = 1, \quad \theta(0) = \theta_M^s,\ \theta(T) = \theta_M^f.$$

This process describes the temperature-induced transition from austenite ($\xi = 0$) to martensite ($\xi = 1$) as the temperature decreases from θ_M^s to θ_M^f (see Fig. 3). Now, at $t = 0$

$$\rho_R \partial_\xi \phi = c_\theta \theta_M^s - c_\tau \tau_0 + c_d = 0.$$

Next ξ increases and θ decreases and then

$$\rho_R \partial_\xi \phi = -\alpha\xi + c_\theta \theta - c_\tau \tau_0 + c_d < 0$$

as $t \in (0, T]$. Thus eq. (27) becomes

$$\dot{\xi} = -k(\theta)\dot{\theta} - \beta(\theta) g(\xi)\, \mathrm{sgn}[\alpha\xi - c_\theta \theta + c_\tau \tau_0 - c_d]\dot{\theta} = -k(\theta)\dot{\theta} - \beta(\theta) g(\xi)\dot{\theta}. \quad (35)$$

Integrating (35) on $(0, T)$ gives the value of θ_M^f. For simplicity let $k(\theta) = k_0$ and $\beta(\theta) g(\xi) = \beta_0 g_0$. Then (35) simplifies to

$$\dot{\xi} = -k_0 \dot{\theta} - \beta_0 g_0 \dot{\theta}. \quad (36)$$

Along the line from θ_M^s to θ_M^f the fraction ξ varies from 0 to 1; integration of (36) then gives

$$\theta_M^f = \theta_M^s - \frac{1}{k_0 + \beta_0 g_0}.$$

On the other hand, along the line from θ_A^s to θ_A^f the fraction ξ varies from 1 to 0 and then integration of (36) yields

$$\theta_A^f = \theta_A^s + \frac{1}{k_0 + \beta_0 g_0}.$$

In light of (31) we can write θ_M^f and θ_A^f in the form

$$\theta_M^f = \frac{\tau_0 - \tau_d}{m} - \frac{1}{k_0 + \beta_0 g_0}, \qquad \theta_A^f = \frac{\tau_0 - \tau_d + q}{m} + \frac{1}{k_0 + \beta_0 g_0}.$$

Note that in order to obtain the loop as depicted in Fig. 3 we need $\theta_M^f(\tau_0) \geq \hat{\theta}_M$ (see also Fig. 5a). Hence it is required that

$$\tau_0 \geq \tau_d + \frac{m}{k_0 + \beta_0 g_0} + m\hat{\theta}_M := \tau_*.$$

Remembering (33) it follows

$$\frac{1}{k_0+\beta_0 g_0} = \theta_* - \hat{\theta}_M. \tag{37}$$

Likewise we can consider the evolution at constant temperature, $\theta = \theta_0$. Consider the line $(\tau,\xi)(t)$ from $(\tau_M^s, 0)$ to $(\tau_M^f, 1)$ (see Fig. 2). Now,

$$\rho_R \partial_\xi \phi = -\alpha\xi + c_\theta\theta - c_\tau\tau + c_d \tag{38}$$

vanishes at $\xi = 0, \tau = \tau_M^s, \theta = \theta_0$. Next ξ and τ increase so that $\partial_\xi\phi < 0$ as $t \in (0, T]$. In view of (28) with $\varkappa(\tau) = \varkappa_0$ and $\nu(\tau)g(\xi) = \nu_0 g_0$, the evolution equation reads

$$-\varkappa_0\dot{\tau} + \dot{\xi} = g_0\nu_0\dot{\tau}.$$

Integration from $t = 0$ to $t = T$ yields

$$\tau_M^f = \tau_M^s + \frac{1}{\varkappa_0+\nu_0 g_0}$$

and likewise

$$\tau_A^f = \tau_A^s - \frac{1}{\varkappa_0+\nu_0 g_0}.$$

Since $\tau_M^s = m\theta_0 + \tau_d$ and $\tau_A^s = m\theta_0 + \tau_d - q$ then we find that

$$\tau_M^f = m\theta_0 + \tau_d + \frac{1}{\varkappa_0+\nu_0 g_0}, \qquad \tau_A^f = m\theta_0 + \tau_d - q - \frac{1}{\varkappa_0+\nu_0 g_0},$$

where $\tau_d = \tau_* - m\theta_*$. The loop can occur in the form depicted in Fig. 2 provided that $\tau_A^f(\theta_0) \geq 0$. Hence it is required that (see also Fig. 5b)

$$\theta_0 \geq \frac{q-\tau_d}{m} + \frac{1}{m(\varkappa_0+\nu_0 g_0)} =: \hat{\theta}_A$$

and from (32)-(33) it follows

$$\frac{1}{\varkappa_0+\nu_0 g_0} = m(\hat{\theta}_A - \theta_\dagger). \tag{39}$$

By construction of the schematic phase diagram in Fig. 5, $\hat{\theta}_A - \theta_\dagger = \theta_* - \hat{\theta}_M$ and then from (37)-(39) it follows $k_0 + \beta_0 g_0 = m(\varkappa_0 + \nu_0 g_0)$.

6.3 An operative example

The operative character of the present approach is now shown by considering particular linear cases.

6.3.1 Temperature-induced transition processes

The austenite-martensite transition, induced by temperature, shows a behaviour like that in Fig. 3. We now show how transitions are obtained through the model equations derived above. Also for numerical convenience we use relative non-dimensional variables and hence the results hold irrespective of the alloy under consideration.

Let $\vartheta = \theta/\hat{\theta}_M$. In view of (27) we consider the evolution equation in the form

$$\dot{\xi} = -k_0\dot{\vartheta} + \gamma_0 \operatorname{sgn}(\xi - \mathcal{S}(\vartheta) + \mathcal{T}(\varsigma_0))|\dot{\vartheta}|,$$

where $k_0 > 0, \gamma_0 := \beta_0 g_0 > 0$, and $\varsigma_0 = \tau_0/\tau_*$, $\tau_0 \geq \tau_*$. An hysteretic loop involves both transitions, from austenite to martensite and vice versa. Note that the saturation property at $\xi = 0$ (during heating) and at $\xi = 1$ (during cooling) is verified only if $\gamma_0 = k_0$.

In Fig. 3 the theoretical description of the loop is represented with its clockwise orientation. Fig. 6, instead, shows the computed major hysteretic loop associated with the data

$$k_0 = 1, \quad \gamma_0 = \begin{cases} 1 \text{ if } 0 \leq \xi \leq 1, \\ 0 \text{ otherwise,} \end{cases} \quad \mathcal{S}(\vartheta) = \vartheta, \quad \mathcal{T}(\varsigma_0) = \tfrac{5}{2}.$$

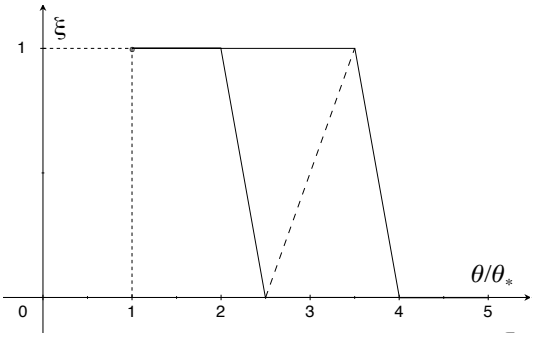

Fig. 6 Major loop of the temperature-induced transition

6.3.2 Stress-induced transition processes

We let $\theta = \theta_0 \geq \hat{\theta}_A$ and describe the evolution of $\tau = \tau_*\varsigma$ and ξ via the linear differential equation (28) that takes the form

$$\dot{\xi} = \varkappa_0\dot{\varsigma} + \delta_0 \operatorname{sgn}[\xi - \mathcal{S}(\vartheta_0) + \mathcal{T}(\varsigma)]|\dot{\varsigma}|, \tag{40}$$

where $\varkappa_0 > 0, \delta_0 := \nu_0 g_0 > 0, \vartheta_0 = \theta_0/\hat{\theta}_A$. Note that the saturation property at $\xi = 0$ (during cooling) and at $\xi = 1$ (during heating) is verified only if $\delta_0 = \varkappa_0$.

While Fig. 2 describes the qualitative hysteretic loop oriented in the counter-clockwise sense, Fig. 7 shows the numerical simulation obtained in the particular case

$$\varkappa_0 = 1, \quad \delta_0 = \begin{cases} 1 \text{ if } 0 \le \xi \le 1, \\ 0 \text{ otherwise,} \end{cases} \quad \mathcal{T}(\varsigma) = \varsigma, \quad \mathcal{S}(\vartheta_0) = \tfrac{7}{2}.$$

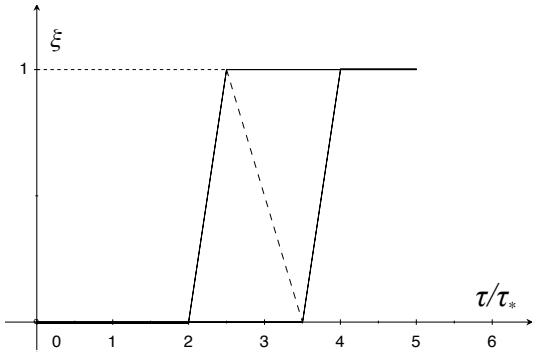

Fig. 7 Major loop of the stress-induced transition

6.3.3 Stress-strain hysteresis at constant temperature (pseudoelasticity)

Let $\theta = \theta_0$ be the constant temperature. In view of (22) we can write the strain variable h in the form

$$h = [\mathcal{T}'(\tau) + \alpha\varkappa(\tau)]\xi - \partial_\tau \mathcal{G}(\tau, \theta_0) - \varkappa(\tau)[\mathcal{S}(\theta_0) - \mathcal{T}(\tau)].$$

We keep regarding $\mathcal{T}(\tau)$ as linear. Furthermore we let $\varkappa$ be constant, $\varkappa(\tau) = \varkappa_0$, and $\partial_\tau \mathcal{G}(\tau, \theta_0)$ be linear in τ. We can then write h in the form $h = \Sigma\tau + \Lambda\xi + \Upsilon$, where $\Sigma, \Lambda, \Upsilon$ are constants, and then

$$\dot{h} = \Sigma\dot{\tau} + \Lambda\dot{\xi}. \tag{41}$$

Using (40) with $\varkappa_0 = \delta_0$ we can determine $\dot{\xi}$ in terms of $\dot{\tau}$. Then substitution in (41) yields

$$\dot{h} = [\Sigma + \delta_0\Lambda/\tau_*]\dot{\tau} + \delta_0(\Lambda/\tau_*)\,\mathrm{sgn}[\xi - \mathcal{S}(\theta_0) + \mathcal{T}(\tau)]|\dot{\tau}|.$$

A numerical simulation of this hysteretic Duhem equation provides loops at constant temperature θ_0 in the stress-strain plane. Finally, a direct interchange of axes results in the sought hysteretic loop in the $h - \tau$ plane (see Fig. 1).

By (23) and (38), the linear approximation of the transition function h^{tr} can be written in the form

$$h^{tr} = \varkappa_0(\alpha\xi + c_\tau\tau - c_\theta\theta - c_d),$$

that exhibits a linear dependence of h^{tr} on ξ, τ and θ. Therefore, even in the linear approximation at constant temperature, the current approach represents a generalization with respect to others present in the literature, in which h^{tr} depends (linearly) only on ξ (see, e.g., [2, 25]).

7 Relation to other approaches

Within the literature on models for SMAs there is a variety of approaches with differences and similarities to the present one. To illustrate the conceptual differences it is natural to consider the pertinent aspects in the corresponding one-dimensional setting.

7.1 Dissipation-consistent modelling

In [26] the generalized stress and strain are decomposed additively in energetic and dissipative parts. The Helmholtz free energy (i.e. energy storage potential in [26]) per unit volume is subject to the dissipation inequality

$$d := -\dot{\Psi} + \tau\dot{h} \geq 0,$$

where d is the dissipation density; in our notation $d = \rho_R\theta\gamma$. Letting $\Psi = \Psi(h, \xi)$ we have

$$-\partial_h\Psi\dot{h} + \tau\dot{h} - \partial_\psi\Psi\dot{\xi} \geq 0.$$

The stress τ is decomposed as the sum

$$\tau = \tau^{en} + \tau^{dis},$$

respectively energetic and dissipative parts. Upon the assumption $\tau^{en} = \partial_h\Psi$ it follows the reduced dissipation inequality

$$d = \tau^{dis}\dot{h} - \partial_\xi\Psi\,\dot{\xi} \geq 0.$$

So far the steps are consistent with the Coleman-Noll and present procedure.

Next X^{en} and X^{dis} are defined by

$$X^{en} := \partial_\xi\Psi, \qquad X^{dis} := -X^{en}$$

and then d can be written in the form

$$d = \tau^{dis}\dot{h} + X^{dis}\dot{\xi} \geq 0.$$

With this form the pair $\mathbf{A} = (\tau^{dis}, X^{dis})$ is said to be the generalized force and $\mathbf{a} = (\dot{h}, \dot{\xi})$ the corresponding velocity. Next, based on the general assumption of normal dissipativity (see, e.g., [27] and refs therein), it is assumed that there exists a convex potential $\varphi(\mathbf{A})$ such that

$$\mathbf{a} \in \partial\varphi(\mathbf{A})$$

where ∂ denotes the sub-differential.

Aside from the convexity requirement, the assumption would amount to considering τ^{dis} and X^{dis} as the variables and $\dot{h}$ and $\dot{\xi}$ as the sought constitutive functions. Even though γ is not allowed to be a constitutive function, we might say that in our approach the derivative $\dot{\xi}$ depends on both the other derivatives (e.g. $\dot{h}$) and the partial derivatives $\partial_h\Psi$, $\partial_\xi\Psi$. This type of dependence is missing in principle within the normal dissipativity.

7.2 Modelling through internal state variables

Among the approaches involving internal state of variables we revisit [24], ch. 3, in the one-dimensional setting. The infinitesimal strain is split in the form $\epsilon = \epsilon^{el} + \epsilon^{tr}$ and the CD inequality is assumed as

$$\sigma\dot{\epsilon} - \rho(\dot{\psi} + \eta\dot{\epsilon}) \geq 0.$$

Next the free energy $\Phi = (\psi - \sigma\epsilon/\rho)$ is considered so that

$$-\rho(\dot{\Phi} + \eta\dot{\theta}) - \epsilon\,\dot{\sigma} \geq 0,$$

possibly letting ρ be constant. Hence, with the variables $\sigma, \theta, \epsilon^{tr}, \xi$ we have

$$-(\epsilon + \rho\partial_\sigma\Phi)\dot{\sigma} - \rho(\partial_\theta\Phi + \eta)\dot{\theta} - \rho\partial_{\epsilon^{tr}}\Phi\dot{\epsilon}^{tr} - \rho\partial_\xi\Phi\dot{\xi} \geq 0.$$

It follows

$$\epsilon = -\rho\partial_\sigma\Phi, \qquad \eta = -\partial_\theta\Phi$$

and

$$\rho\partial_{\epsilon^{tr}}\Phi\dot{\epsilon}^{tr} + \rho\partial_\xi\Phi\dot{\xi} \leq 0.$$

Thanks to the particular free energy

$$\Phi = -\frac{1}{2\rho}\mathcal{S}\sigma^2 - \frac{1}{\rho}\sigma[\alpha(\theta - \theta_0) + \epsilon^{tr}] + c[\theta - \theta_0 - \theta\ln(\theta/\theta_0)] - \eta_0\theta + \Phi_0 + \frac{1}{\rho}f(\xi)$$

we have

$$\partial_{\epsilon^{tr}}\Phi = -\frac{1}{\rho}\sigma$$

and then the inequality can be written

$$\sigma\dot{\epsilon}^{tr} - \rho\partial_{\xi}\Phi\dot{\xi} \geq 0. \tag{42}$$

At constant temperature, $\dot{\theta} = 0$, equation (42) appears to be similar to (11) once we recall that $\gamma \geq 0$. Yet the procedure in [24] does not determine evolution equations on the basis of (42). Rather it is postulated that

$$\dot{\epsilon}^{tr} = \Lambda\dot{\xi}$$

with an ad hoc assumption on Λ and an appropriate parameterization depending on the sign of $\dot{\xi}$.

7.3 A model involving a generalized surface force

An apparently different approach is developed in [10] through a nonlocal scheme. Without entering the details we mention that the balance of energy, and then the CD inequality, is changed by allowing for a surface force density Q conjugate to $\dot{\xi}$ in that the corresponding power density is $Q\dot{\xi}$ though without affecting the balance of linear momentum; in three dimensions the surface power density is $\mathbf{Q}\dot{\xi}\cdot\mathbf{n}$ and $\nabla\cdot(\mathbf{Q}\dot{\xi})$ is the corresponding power per unit volume. The heat conduction inequality is set aside and then the CD inequality becomes

$$\sigma\dot{\epsilon} - \rho(\dot{\psi} + \eta\dot{\theta}) + \partial_x(Q\dot{\xi}) \geq 0, \tag{43}$$

x being the Cartesian coordinate. Accordingly $Q\dot{\xi}$ may be viewed as an extra-entropy flux. To account for nonlocality also $\partial_x\xi$ is a variable in addition to ϵ, θ, ξ. Consequently the CD inequality (43) yields

$$-\rho(\partial_{\theta}\psi + \eta)\dot{\theta} + \sigma\dot{\epsilon} - \rho\partial_{\epsilon}\psi\dot{\epsilon} - \rho\partial_{\partial_x\xi}\psi(\partial_x\xi)^{\cdot} + \partial_x(Q\dot{\xi}) \geq 0.$$

The classical relation $\eta = -\partial_{\theta}\psi$ follows. Now, since $\partial_x(Q\dot{\xi}) = (\partial_x Q)\dot{\xi} + Q\partial_x\dot{\xi}$ and, in the linear approximation,

$$(\partial_x\xi)^{\cdot} = \partial_x\dot{\xi} - \partial_x\xi\dot{\epsilon}.$$

The remaining inequality has the form

$$[\sigma - \rho(\partial_{\epsilon}\psi + \partial_{\partial_x\xi}\psi\,\partial_x\xi)]\dot{\epsilon} + (\partial_x Q - \rho\partial_{\xi}\psi)\dot{\xi} + (Q - \rho\partial_{\partial_x\xi}\psi)\partial_x\dot{\xi} \geq 0.$$

Next letting $\sigma = \sigma^e + \sigma^d$, and allowing σ^d depend also on $\dot{\epsilon}$ ref. [10] arrives to the dissipation inequality

$$\rho\delta = \sigma^d\dot{\epsilon} + X\dot{\xi} \geq 0,$$

where

$$X = -\rho\partial_{\xi}\psi + \partial_x(\rho\partial_{\partial_x\xi}\psi),$$

and possibly split in

$$\sigma^d \dot{\epsilon} \geq 0, \qquad X\dot{\xi} \geq 0.$$

The evolution of ξ is then established by letting

$$\dot{\xi} = L\, X,$$

L being a positive constant.

7.4 Models based on the Ginzburg-Landau theory

It is worth mentioning Falk's model ([28, 29]; [6], ch. 5) which is based on the analogy with Landau-Devonshire form of the free energy for hysteretic materials. The free energy is assumed in the form

$$\psi(\theta, F) = \psi_0(\theta) + \alpha_1(\theta - \theta_0)F^2 - \alpha_2 F^4 + \alpha^3 F^6,$$

where $\alpha_1, \alpha_2, \alpha_3$ are positive constants. The body is thought as a stack of layers and then to account for interfacial energies a term $\frac{1}{2}\nu(\partial_x F)^2$ is comprised in the internal energy. Hence the total free energy is considered in the form

$$\psi_{tot} = \psi(\theta, F) + \tfrac{1}{2}\nu(\partial_x F)^2 - \rho b u$$

while $\frac{1}{2}\rho(\partial_t u)^2$ is the kinetic energy density. Next Hamilton's principle is applied and the equation of motion is obtained in the form

$$\rho\partial_t^2 u - \partial_x\partial_F\psi(\theta, F) + \nu\partial_x^4 u = \rho b(x, t), \tag{44}$$

where $x \in [0, 1]$ and $t > 0$. Among the conceptual differences, (44) is a fourth-order equation in the displacement u via the term $\nu\partial_x^4 u$. In addition the evolution of the temperature is governed by the classical Fourier scheme.

In the framework of a Ginzburg-Landau-Devonshire theory, the minimum (Gibbs) free energy representation has been obtained in [25] as a quadratic function of the stress σ and the anelastic deformation h^{tr}. The temperature is regarded as a given parameter. This approach involves an order parameter φ whose modulus represents the martensitic mass fraction, namely $\xi = |\varphi|$. In addition, the anelastic deformation h^{tr} is represented as a quadratic function of φ^2, so that the free energy turns out to be an eighth-order function of φ. This approach allows to highlight the role of the Ginzburg-Landau equation when phase transitions occur in materials with hysteresis such as SMAs.

8 Conclusions

Within the wide literature on the modelling of SMAs we can distinguish among microscopic and macroscopic models (see, e.g. [3]). Microscopically, a strain measure is considered which is based on interatomic potentials. Macroscopic approaches are based on a free energy function of temperature and strain, the strain being decomposed in elastic and transformation parts $\boldsymbol{\epsilon}^e, \boldsymbol{\epsilon}^{tr}$. Conceptually the macroscopic approaches are characterized by the modelling of the transformation strain $\boldsymbol{\epsilon}^{tr}$; some ways are mentioned in sec. 6. In essence we can say that macroscopically the mass fraction ξ of a constituent (e.g. martensite) is considered and the constitutive properties emerge from a free energy potential while the transition strain $\boldsymbol{\epsilon}^{tr}$ is eventually related to the ξ through a properly-defined rate equation.

In the present approach the constitutive equations depend on the temperature θ, the one-dimensional stress τ, the mass fraction ξ, and the derivatives $\dot{\theta}, \dot{\tau}$ while $\dot{\xi}$ is given by a constitutive rate equation. The main novelty of our approach is that the entropy production density (here γ) is itself given by a constitutive function (of $\theta, \tau, \xi, \dot{\theta}, \dot{\tau}$). For simplicity the model is one-dimensional and the strain variable is $h = \ln F$, with F the deformation derivative in the longitudinal direction. Within this non-linear theory the whole set of thermodynamic restrictions is derived. Next a free energy function ϕ is considered in the form (16). Hence we find that

$$0 = \rho_R \partial_\xi \phi = -\alpha\xi + \mathcal{S}(\theta) - \mathcal{T}(\tau),$$

here referred to as skeleton surface, characterizes the equilibrium mixed states (θ, τ, ξ). Meanwhile, upon the selection of the constitutive function (24) for the entropy production, the evolution condition for ξ is obtained in the form (26).

The operative aspect of the theory is emphasized in section 6 by using a linearized version of the equations so that their integration can be done in closed form. Hence detailed hysteretic loops are derived according as they are induced by temperature or by stress. Note that some characteristic parameters of the model, $k_0, \varkappa_0, \tau_d, q$, are related to experimentally measurable quantities such as $m, \theta_*, \tau_*, \theta_\dagger, \hat{\theta}_M, \hat{\theta}_A$.

A further development along the lines of this paper is the generalization to bodies subject to fields within a three-dimensional setting.

References

1. P.K. Kumar, D.C. Lagoudas, Introduction to Shape Memory Alloys, in: Shape Memory Alloys: Modeling and Engineering Applications, D.C. Lagoudas Ed., Springer, New York, 2008
2. L. Xu, T. Baxevanis, D.C. Lagoudas, A three-dimensional constitutive model for the martensitic transformation in polycrystalline shape memory alloys under large deformation, Smart Mater. Struct. 28, 074004 (2019)
3. C. Cisse, W. Zaki, T. Ben Zineb, A review of constitutive models and modeling techniques for shape memory alloys, Int. J. Plasticity 76, 244-284 (2016)

4. Brinson, L.C. One dimensional constitutive behavior of shape memory alloys: Thermomechanical derivation with nonconstant material functions and redefined martensite internal variable. J. Intell. Mater. Syst. Struct. 1993, 4, 229-242
5. Y. Huo, I. Müller, Nonequilibrium thermodynamics of pseudoelasticity, Cont. Mech. Thermodyn. 5, 163-204 (1993)
6. M. Brokate, J. Sprekels, Hysteresis and Phase Transitions, Springer, New York, 1996
7. Seelecke, S.; Müller, I. Shape memory alloy actuators in smart structures: Modeling and simulation. Appl. Mech. Rev. 2004, 57, 23-46
8. G. Scalet, F. Niccoli, C. Garion, P. Chiggiato, C. Maletta, F. Auricchio, A three-dimensional phenomenological model for shape memory alloys including two-way shape memory effect and plasticity, Mech. Mater. 136, 103085 (2019)
9. Y. Jin, A. Artemev, A. Khachaturyan, Three-dimensional phase-field model of low-symmetry martenitic transformation in polycrystal: simulation of $\zeta_2$martensite in AuCd alloys, Acta Mater. 49, 2309-2320 (2001)
10. V.I. Levitas, Thermodynamically consistent phase field approach to phase transformations with interface stresses, Acta Mater. 61, 4305-4319 (2013)
11. A. Morro, C. Giorgi, Techniques for the thermodynamic consistency of constitutive equations, *Thermo*, 3 (2023) 260-276.
12. C. Giorgi, A. Morro, On the second law of thermodynamics in continuum physics, *Thermo*, 4 (2024), 273-294.
13. C. Giorgi, A. Morro, Strain-rate and stress-rate models of nonlinear viscoelastic materials, *Mathematics* 12 (2024) 3011.
14. C. Truesdell, R.A. Toupin, The classical field theories, in Encyclopedia of Physics, vol. III/1, ed. S. Flügge (Springer, Berlin, 1960
15. A.C. Eringen, Mechanics of Continua, Wiley, New York, 1967
16. M.E. Gurtin, E. Fried, L. Anand, The Mechanics and Thermodynamics of Continua, Cambridge University Press, 2010
17. A. Morro, C. Giorgi, Mathematical Modelling of Continuum Physics, Birckhäuser, Cham, 2023
18. W. Dreyer, C. Guhlke, M. Herrmann, Hysteresis and phase transition in many-particle storage systems Cont. Mech. Thermodyn. 23, 211-231 (2011)
19. X. Wu, G. Sun, J. Wu, The nonlinear relationship between transformation strain and applied stress for nitinol, Mater. Lett. 57 (2003) 1334-1338
20. E.E. Timofeeva et al., On the stress-temperature dependences in TiNi-based shape memory alloys, J. Alloys Compd., 905 (2022) 164227.
21. E. Abel, L. Hongyan, M. Pridham, A. Slade. Issues concerning the measurement of transformation temperatures of NiTi alloys. Smart Mater. Struct., 13 (2004) 1110.
22. T. Gottschall et al. On the S(T) diagram of magnetocaloric materials with first-order transition: Kinetic and cyclic effects of Heusler alloys, Acta Mater. 107 (2016) 1-8
23. M. A. Mandolino, D. Scholtes, F. Ferrante and G. Rizzello. A Physics-Based Hybrid Dynamical Model of Hysteresis in Polycrystalline Shape Memory Alloy Wire Transducers, in IEEE/ASME Transactions on Mechatronics (TMECH), 28 (2023) 2529-2540.
24. D.C. Lagoudas ed., Shape Memory Alloys. Modeling and Engineering Applications. Springer, New York, 2008
25. A. Berti, C. Giorgi, E. Vuk, Free energies and pseudo-elastic transitions for shape memory alloys, Discrete Contin. Dyn. Syst. Ser. S, 6 (2013) 293-316.
26. A.T. McBride, B.D. Reddy, P. Steinmann, Dissipation-consistent and classification of extended plasticity formulations, J. Mech. Phys. Solids 119, 118-139 (2018)
27. B. Halphen, N. Quoc Son, Sur les matériaux standards généralisés, J. Mécan. 14, 39-63 (1975)
28. F. Falk, Landau theory and martensitic phase transitions, J. Physics C 12, 3-15 (1982)
29. F. Falk, One-dimensional model of shape memory alloys, Arch. Mech. 35, 63-84 (1983)